6. In this event, the ester alkyl chain of the (S)-analyte and the alkyl chain at the chiral center of the (R)-analyte were oriented to intercalate between the adjacent strands of the bonded phase, influence the stability difference between the two diastereomeric (S,S)- and (R,S)-complex and consequently control the separation factor according to the length of the ester alkyl chain and to the length of the alkyl chain at the chiral center of the analyte. The chromatographic resolution trends for resolving a homologous series of N-acyl-α-(1-naphthyl)alkylamine **6** and a homologous series of N-(3, 5-dinitrobenzoyl)-α-amino alkyl ester **7** expected from the chiral recognition models shown in Figure 3 and 6 were found to be exactly consistent with those observed. Therefore it might be concluded that the chiral recognition models proposed in this study are quite convincing. However, it should be noted that the chiral recognition models proposed in this study might be modified or improved as more data relevant to the chromatographic resolution are collected.

Acknowledgment. This work was supported by OCRC-KOSEF and Basic Science Research Institute Program (BSRI-96-3410).

References

1. (a) Krstulovic, A. M. Ed. *Chiral Separations By HPLC: Applications to Pharmaceutical Compounds*; Ellis Horwood: Chichester, England, 1989. (b) Ahuja, S. Ed. *Chiral Separations by Liquid Chromatography*; ACS Symposium Series 471, American Chemical Society: Washington, DC. 1991. (c) Taylor, D. R.; Maher, K. *J. Chromatogr. Sci.* **1992**, *30*, 67.
2. For example, see Perrin, S. R.; Pirkle, W. H. In *Chiral Separations by Liquid Chromatography*; Ahuja, S., Ed.; ACS Symposium Series 471, American Chemical Society: Washington, DC. 1991; chap. 3.
3. (a) Pirkle, W. H.; Finn, J. M.; Schreiner, J. L.; Hamper, B. C. *J. Am. Chem. Soc.* **1981**, *103*, 3964. (b) Hyun, M. H.; Kim, M. H. *J. Liq. Chromatogr.* **1990**, *13*, 3229. (c) Hyun, M. H.; Cho, Y. J.; Min, C.-S.; Ryoo, J.-J. *Bull. Kor. Chem. Soc.* **1995**, *16*, 764.
4. (a) Pirkle, W. H.; Hyun, M. H.; Bank, B. *J. Chromatogr.* **1984**, *316*, 585. (b) Hyun, M. H.; Park, Y.-W.; Baik, I.-K. *Tetrahedron Lett.* **1988**, *29*, 4735. (c) Hyun, M. H.; Cho, Y. J.; Ryoo, J.-J.; Jyung, K. K.; Heo, G. S. *J. Chromatogr. A.* **1995**, *696*, 173. (d) Hyun, M. H.; Lee, J. B. *Bull. Kor. Chem. Soc.* **1995**, *16*, 977.
5. (a) Hyun, M. H.; Pirkle, W. H. *J. Chromatogr.* **1987**, *393*, 357. (b) Oi, N.; Kitahara, H.; Matsumoto, Y.; Nakajima, H.; Horikawa, Y. *J. Chromatogr.* **1989**, *462*, 382. (c) Tambute, A.; Siret, L.; Caude, M.; Begos, A.; Rosset, R. *Chirality*, **1990**, *2*, 106. (d) Hyun, M. H.; Jin, J. S.; Ryoo, J.-J.; Jyung, K. K. *Bull. Kor. Chem. Soc.* **1994**, *15*, 497. (e) Hyun, M. H.; Jin, J. S.; Na, M. S.; Jyung, K. K. *Bull. Kor. Chem. Soc.* **1995**, *16*, 344.
6. Hyun, M. H.; Min, C.-S. *Chem. Lett.* **1994**, 1463.
7. Hyun, M. H.; Ryoo, J.-J.; Min, C.-S. *Bull. Kor. Chem. Soc.* **1992**, *13*, 407.
8. (a) Pirkle, W. H.; Murray, P. G.; Burke, J. A. *J. Chromatogr.* **1993**, *641*, 21. (b) Hyun, M. H.; Min, C. S.; Cho, Y. J.; Na, M. S. *J. Liq. Chromatogr.* **1995**, *18*, 2527.
9. Hyun, M. H.; Cho, S. M.; Ryoo, J.-J.; Kim, M. S. *J. Liq. Chromatogr.* **1994**, *17*, 317.

Synthesis, Crystal Structure, and Magnetic Properties of RbV_2SeO_7 as Compared with KV_2SeO_7

Yoon Hyun Kim, Young-Uk Kwon*, and Kyu-Seok Lee

Department of Chemistry, Sung Kyun Kwan University, Suwon 440-746, Korea

Received August 1, 1996

Crystalline compound RbV_2SeO_7, a Rb analogue of KV_2SeO_7, was synthesized from a hydrothermal reaction of V_2O_5, V_2O_3, SeO_2, and Rb_2CO_3 in the mole ratio 3 : 1 : 15 : 6 (in millimoles) at 230 ℃. RbV_2SeO_7 crystallizes in an orthorhombic space group *Pnma* (No. 62) with $a=18.444(8)$, $b=5.415(3)$, $c=7.070(4)$ Å, $Z=8$. The two structures of KV_2SeO_7 and RbV_2SeO_7 are almost the same except that bond lengths in the latter are slightly longer than in the former. The magnetic susceptibility measurement for RbV_2SeO_7 in the temperature range 4-300 K showed an antiferromagnetic ordering with $T_N=45$ K, higher than that for KV_2SeO_7 of 27 K. The origin of the magnetic coupling and the different ordering temperatures in the two phases are discussed in relation to the crystal structures.

Introduction

Recently, one can find increasing number of publications on the hydrothermal reactions applied to synthesize novel inorganic compounds.[1] This technique is considered as one of the low-temperature synthesis techniques from which compounds with interesting structures and physical properties are often obtained.

During our investigation into the hydrothermal reactions in the vanadium selenite system, we have synthesized a mixed valent layered compound KV_2SeO_7.[2] This compound showed an antiferromagnetic ordering at 27 K whose susceptibility

Table 1. Crystal data and structure refinement for RbV_2SeO_7

Formula weight	378.30
Temperature	293(2) K
Wavelength	0.71073 Å
Space group	*Pnma* (No. 62)
Unit cell dimensions (Å)	$a=18.444(8)$
	$b=5.415(3)$
	$c=7.070(4)$
Volume	706.1(6) Å^3
Z	4
Absorption coefficient	146.37 cm^{-1}
Crystal size	0.1×0.15×0.3 mm
Goodness-of-fit on F^2	1.136
R indices (all data)	$R_1^a=0.0639$, $wR_2^b=0.1537$
Largest diff. peak and hole	1.363 and −1.387 e.Å^{-3}

$^aR_1=\sum||F_o|-|F_c||/\sum|F_o|$. $^bwR_2=[\sum|w(F_o^2-F_c^2)^2|/\sum|w(F_o^2)^2|]^{1/2}$ with $w=1/[\sigma^2(Fo^2)+(0.0936P)^2+11.24P]$, where $P=(Fo^2+2Fc^2)/3$.

Table 2. Atomic coordinates (×10^4) and equivalent isotropic displacement parameters (Å^2×10^3) for RbV_2SeO_7

	x	y	z	U(eq)^a
Rb	344(1)	2500	2541(2)	16(1)
Se	3468(1)	2500	145(2)	8(1)
V(1)	3128(1)	2500	−4417(3)	6(1)
V(2)	1220(1)	2500	7683(3)	6(1)
O(1)	2268(6)	2500	6223(17)	23(3)
O(2)	1664(5)	8(17)	9317(12)	36(2)
O(3)	1322(6)	−2500	2755(15)	28(3)
O(4)	988(4)	−118(12)	5723(10)	15(2)
O(5)	410(6)	2500	−1442(15)	19(3)

$^aU(eq)=1/3\ (U_{11}+U_{22}+U_{33})$.

vs. temperature curve could be well accounted for with the 1D-Heisenberg model for S=1/2. The origin of the 1D coupling was explained, based on the crystal structure, as due to superexchange between the 3d-orbitals of V *via* the 2p-orbitals of intervening oxygen atoms.[3]

Magnetic coupling mechanism has been an ever intriguing problem to chemists and physicist. Although there are a numerable comprehensive articles on this issue, experimental confirmation of the theory is far from satisfaction.[4]

In order to understand the magnetism in more detail, we have attempted to synthesize a Rb analogue of KV_2SeO_7. Some changes in the structural parameters were expected from those of KV_2SeO_7, and we were interested in the effect of such changes on the magnetic properties.

In this paper, we report on the synthesis, crystal structure of RbV_2SeO_7 and compare its magnetic properties with those of KV_2SeO_7. We also discuss on the influence of the structure on the magnetic ordering temperature in this structure.

Experimental

Table 3. Selected Bond Distances (Å) and Angles (deg) for KV_2SeO_7 and RbV_2SeO_7

	RbV_2SeO_7	KV_2SeO_7
A-O(5)	2.819(11)	2.723(8)
A-O(4)×2	2.913(7)	2.823(8)
A-O(4)′×2	3.033(8)	2.907(7)
A-O(5)×2′	3.141(6)	3.120(5)
A-O(3)×2	3.257(7)	3.176(6)
V(1)-O(1)	1.650(11)	1.643(9)
V(1)-O(2)×2	1.671(8)	1.640(9)
V(1)-O(3)	1.841(11)	1.802(9)
V(2)-O(5)	1.617(10)	1.603(9)
V(2)-O(2)×2	1.956(8)	1.952(8)
V(2)-O(4)×2	2.028(7)	2.012(8)
V(2)-O(1)	2.191(11)	2.192(9)
Se-O(4)×2	1.684(7)	1.669(6)
Se-O(3)	1.734(11)	1.732(10)
O(1)-V(1)-O(2)	111.6(4)	111.4(3)
O(1)-V(1)-O(3)	107.5(6)	107.9(5)
O(2)-V(1)-O(2)	108.7(7)	108.6(8)
O(2)-V(1)-O(3)	108.7(4)	108.8(4)
O(5)-V(2)-O(2)	99.2(4)	99.7(4)
O(2)-V(2)-O(2)	87.2(6)	87.3(7)
O(5)-V(2)-O(4)	93.8(4)	94.9(3)
O(2)-V(2)-O(4)	90.6(3)	90.5(4)
O(4)-V(2)-O(4)	88.7(4)	87.9(4)
O(2)-V(2)-O(1)	84.8(4)	83.8(3)
O(4)-V(2)-O(1)	82.2(3)	81.6(3)
O(5)-V(2)-O(1)	174.4(5)	175.2(5)
O(4)-Se-O(4)	99.9(5)	100.5(5)
O(4)-Se-O(3)	95.9(3)	95.7(3)
V(1)-O(1)-V(2)	167.8(7)	167.0(6)
V(1)-O(2)-V(2)	166.6(6)	166.1(6)
Se-O(3)-V(1)	133.6(7)	135.3(6)
Se-O(4)-V(2)	125.1(4)	124.3(3)

Pure dark-red crystalline phase of RbV_2SeO_7 was prepared from a hydrothermal reaction of V_2O_5, V_2O_3, SeO_2, and Rb_2CO_3 in the mole ratio of 3 : 1 : 15 : 6 (also in millimoles). Details of the reaction condition were described previously.[2]

The crystal structure of RbV_2SeO_7 was determined from single crystal X-ray diffraction data. Room temperature intensity data were collected using 2θ-ω scan method up to 2θ=46°on an Enraf-Nonius CAD4 diffractometer equipped with monochromated Mo Kα(λ=0.71073 Å) radiation. The angle data of twenty five randomly located reflections were indexed to an orthorhombic cell with $a=18.444(8)$, $b=5.415(3)$ and $c=7.070(4)$ Å, V=706.1(6) Å^3, similar to those of KV_2SeO_7. The systematic absence conditions (*0kl*, $k+l=2n$; *hk0*, $h=2n$; *0k0*, $k=2n$; *00l*, $l=2n$) conform to the space group *Pnma* (No. 62) indicating that this Rb-phase is isostructural to KV_2SeO_7 phase. The intensity data were corrected for Lorentz and polarization factors. Absorption corrections were made with DIFABS program[5] (corrections; min. 0.667; max. 1.566;

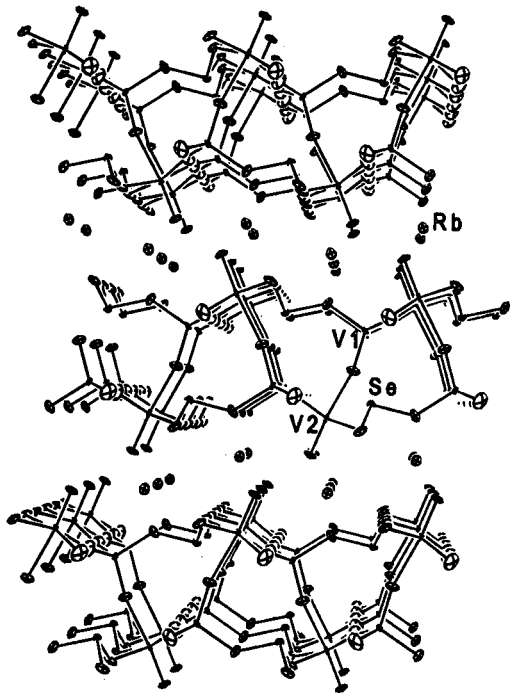

Figure 1. Structure of RbV_2SeO_7 viewed into the [010] direction. Oxygen labels are omitted for clarity.

ave. 1.005). The crystal structure refinements were performed by using SHELXL-93 program[6] with the parameters for KV_2SeO_7 as the starting model. Anisotropic thermal parameters for all atoms were included. The full-matrix least-squares refinements on all F^2 data finally converged to $R_1=0.0639$ and $wR_2=0.1537$ (on F^2).

The crystallographic data, the atomic positional and isotropic thermal parameters, and important bond distances and angles for RbV_2SeO_7 are given in Tables 1, 2, and 3, respectively.

Magnetization data in the temperature range of 4-300 K were obtained with SQUID with a magnetic field of 500 G. Powdered sample was encapsulated in a diamagnetic container for the measurements.

Thermogravimetric (TG) analysis was carried out with a Perkin-Elmer TGA-7 under N_2 flowing. Weight losses of 0.63 % and 29.24% were observed at 380 ℃ and 490 ℃, respectively. The total weight loss of 29.87% was close to the theoretical value of 29.33% corresponding to SeO_2 loss per formula unit.

Results and Discussion

We have previously reported on the synthesis, structure and magnetic properties of KV_2SeO_7.[2] In that paper, we noted that its Rb analogue, RbV_2SeO_7, also could be synthesized although the synthesis conditions were not optimized and the crystallinity of the compound was very poor. It might be due to that the RbOH we used was an aqueous solution which precluded accurate measurements in our experimental scale which, in turn, caused a loss of control over the pH. Slight variations of the pH sometimes lead to dramatic effects on the final products in hydrothermal reactions.[7] Therefore, we used Rb_2CO_3 instead of RbOH because Rb_2CO_3 powder could be handled much more easily. A good yield (80% based on vanadium metal) of crystalline single-phase product was obtained when V_2O_5, V_2O_3, SeO_2, and Rb_2CO_3 were reacted in the mole ratio of 3 : 1 : 15 : 6 at 230 ℃.

The mole ratio, initial average oxidation state of vanadium, and reaction temperature are very important in order to synthesize pure product. When the amount of Rb_2CO_3 was decreased below 6 mmol, impurity phases of unknown nature

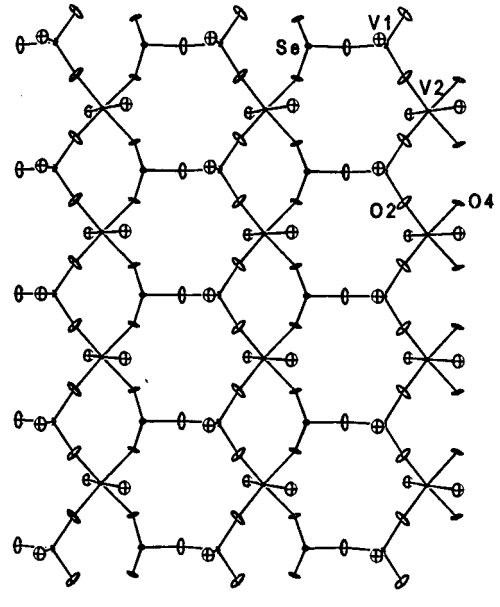

Figure 2. Structure of $[V_2SeO_7]^-$ layer of RbV_2SeO_7 viewed into the [100] direction.

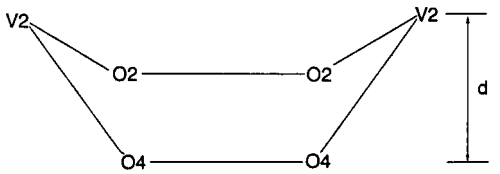

Figure 3. Schematic drawing of the $[V_2O_4]$ unit. Normal distance (d) from vanadium atom to the oxygen plane is shown..

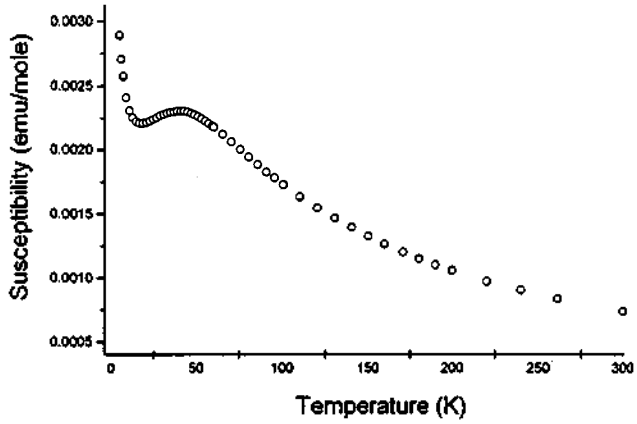

Figure 4. Magnetic susceptibility *vs.* temperature plot for RbV_2SeO_7.

started to form. In contrast, when the Rb_2CO_3 content was increased, green crystals presumably $RbVSe_2O_7H$, a Rb analogue of $KVSe_2O_7H$,[8] were obtained along with RbV_2SeO_7. When even larger amount of Rb_2CO_3 was used to make the solution pH beyond 6, a V(V) compound $RbVSeO_5$ was obtained as the major product. If the reactions were run at below 230 ℃, a large amount of impurity phases formed. The average oxidation state of vanadium in the starting mixture was fixed at +4.5, the same as that of the final product.

In the TG analysis, weight loss occurred by two steps which is reminiscent of KV_2SeO_7 whose synthesis often accompanies with $KVSe_2O_7H$ formation. A typical TG diagram for KV_2SeO_7 showes two weight loss steps at 360 ℃ by 1.4% and 520 ℃ by 30.9% of which the first one coincides with the decomposition temperature of $KVSe_2O_7H$. Therefore, the smaller weight loss step at lower temperature from RbV_2SeO_7 sample is probably due to $RbVSe_2O_7H$ impurity. Counting this as an impurity signal, the purity of our sample would be 98% in weight.

The details of the crystal structure of AV_2SeO_7 (A=K and Rb) are described previously and, in this paper, we will only focus on the part of the structure that is relevant to the magnetic properties of these compounds.[2] There are layers of $[V_2SeO_7]^-$ composed of corner sharing VO_4 tetrahedral, VO_6 octahedral and SeO_3 pyramidal unit (see Figure 1). The two structures are essentially the same. RbV_2SeO_7 has slightly longer bond distances by 0.01-0.02 Å and slightly different bond angles than KV_2SeO_7. Important bond lengths and bond angles of these two compounds are compared in Table 3. Bond valence sum calculations[9] and the common knowledge of coordination chemistry of vanadium metal suggest that the tetrahedral V1 is V^{5+} and the octahedral V2 is V^{4+}. The magnetic V2 atoms are linked to one another within the layers *via* oxygen atoms, O2 and O4 of neighboring VO_6 and SeO_3 units, to form an 1D chain along the b-axis (Figure 2). The V2-V2 separations, same as the b-parameters, are 5.360(3) and 5.415(3) Å for KV_2SeO_7 and RbV_2SeO_7, respectively. These values are too large to allow any significant magnetic interactions between these V atoms. The KV_2SeO_7 compound showed an antiferromagnetic ordering below 27 K and we explained the magnetic curve in terms of 1D-Heisenberg model for S=1/2.[10] The mechanism of the magnetic ordering was attributed to the superexchange mechanism mediated by the four intervening oxygen atoms between vanadium atoms (see Figure 3).

Magnetic susceptibility *vs.* temperature plot for RbV_2SeO_7 is given in Figure 4. There is a broad maximum at about 45 K, higher than 27 K for KV_2SeO_7. If the magnetic ordering is due to direct V-V interactions, T_N for KV_2SeO_7 with the shorter V-V distance, should be higher than that for the RbV_2SeO_7 which is the opposite to the observations. As previously mentioned, the magnetic coupling in these compounds can be explained with the superexchange theory. In our compounds, this mechanism appears to operate through V2-O2-O2-V2 and/or V2-O4-O4-V2 linkages. The strength of the magnetic interactions must be a function of orbital overlaps along these linkages. As an indirect measure of such interaction, we have calculated the normal distances from the V2 atom to the plane defined by the four oxygen atoms (see Figure 3). These values are 0.251(6) Å for KV_2SeO_7 and 0.221 (6) for RbV_2SeO_7. Although the difference is small, RbV_2SeO_7 has more favorable atomic arrangement for magnetic interaction which agrees with the observations. Supporting evidences for the foregoing discussion can be obtained from other vanadium (IV) selenites with the similar principal structure, that is, atomic connectivity. $KVSe_2O_7H$ which shows T_N at 21 K has the normal distance of 0.535(5) Å[8] and $Ba(VO)_2(SeO_3)_2(HSeO_3)_2$ which has normal distances 1.262 and 0.091 Å shows no magnetic ordering down to 4 K.[11]

However, since we did not take bond distances into consideration in above discussion, we cannot take the normal distance as a quantitative measure for T_N. Detailed molecular orbital calculations for these structures will be necessary. It is suggested that the square of energy difference between HOMO and LUMO is inversely proportional to T_N in magnetic coupling.[12] Further theoretical studies are called for.

The high temperature susceptibility data of 50 K<T<300 K could be fitted to Curie-Weiss law $\chi=C/(T+\theta)$, with C= 0.276 Kcm^3/mol, and $\theta=-63$ K. The magnetic moment for the paramagnetic temperature region is $\mu_{eff}=1.46$ BM, smaller than spin only value of d^1 electron, 1.73, and also smaller than the spin-orbit value of 1.68-1.78.[13] There must be some diamagnetic impurity in our sample which is responsible for the small μ_{eff}. Contamination by V^{5+} impurities in our sample seems to be likely because V_2O_5 has been utilized as a starting material. The upturn of susceptibility curve at lower temperature may be due to either paramagnetic impurities or anisotropy of magnetic coupling.

In conclusion, we have synthesized and determined the structure of RbV_2SeO_7, a Rb analogue of the layered mixed valent KV_2SeO_7. There are only small changes in bond distances and angles in the two structures. However, the antiferromagnetic ordering temperature is significantly influenced by such a small structural change to raise T_N from 27 to 45 K. We correlated the shift of T_N with the movement of V^{4+} atom toward the plane of bridging oxygen atoms by as small as 0.030 Å from 0.251 in KV_2SeO_7 and to 0.221 Å in RbV_2SeO_7.

Acknowledgment. We thank the Korean Science and Engineering Foundation (KOSEF 951-0303-003-2) for the financial support.

References

1. (a) Rabenau, A. *Angew. Chem. Int. Ed. Engl.* **1985**, *24*, 1026. (b) Davis, M. E.; Lobo, R. F. *Chem. Mater.* **1992**, *4*, 756.
2. Lee, K.-S.; Kwon, Y.-U.; Namgung, H.; Kim, S.-H. *Inorg. Chem.* **1995**, *34*, 4178.
3. Buffat, B.; Demazeau, G.; Pouchard, M.; Dance, J. M.; Hagenmuller, P. *J. Solid State Chem.* **1983**, *50*, 33.
4. Carlin, R. L. *Magnetochemistry*; Springer-Verlag, Berling Heidelberg: 1986.
5. Walker, N.; Stuart, D. *Acta Crystallogr.* **1983**, *A39*, 158.
6. Sheldrick, G. M. SHELXL-93 User's Guide. Crystallographic Department, University of Gottingen, Germany, 19 93.
7. Kwon, Y.-U.; Lee, K.-S.; Kim, Y. H. *Inorg. Chem.* **1996**, *35*, 1161.
8. Kim, Y. H.; Lee, K.-S.; Kwon, Y.-U.; Han, O. H. *Inorg.*

Chem. **1996**, *35*, accepted.
9. Brown, I. D.; Altermatt, D. *Acta Crystallogr.* **1985**, *B41*, 244.
10. Hatfield, W. E. *J. Appl. Phys.* **1981**, *52*, 1985.
11. Harrison, W. T. A.; Vaughey, J. T.; Jacobson, A. J.; Goshorn, J. W. *J. Solid State Chem.* **1995**, *116*, 77.
12. Whangbo, M. H. private communication.
13. Banerjea, D. *Coordination Chemistry*; McGraw-Hill: Delhi, 1993, p 212.

Dioxygen Binding to the Singly Alkoxo-Bridged Diferrous Complex: Properties of $[Fe^{II}_2(N\text{-Et-HPTB})Cl_2]BPh_4$

Eunsuk Kim†, Kang-Bong Lee‡, and Ho G. Jang†*

Contribution from the †Department of Chemistry, Korea University, Seoul 136-701, Korea
‡Advanced Analysis Center, KIST, Seoul 136-130, Korea
Received August 1, 1996

$[Fe^{II}_2(N\text{-Et-HPTB})Cl_2]BPh_4$ (**1**), where *N*-Et-HPTB is the anion of *N,N,N',N'*-tetrakis(*N*-ethyl-2-benzimidazolylmethyl)-2-hydroxy-1,3-diaminopropane, has been synthesized to model dioxygen binding to the diferrous centers of proteins. **1** has a singly bridged structure with a μ-alkoxo of *N*-Et-HPTB and contains two five-coordinate iron(II) centers with two chloride ligands as exogenous ligands. **1** exhibits an electronic spectrum with a λ_{max} at 336 nm in acetone. **1** in acetone exhibits no EPR signal at 4 K, indicating diiron(II) centers are antiferromagnetically coupled. Exposure of acetone solution of **1** to O_2 at −90 ℃ affords an intense blue color intermediate showing a broad band at 586 nm. This absorption maximum of the dioxygen adduct($1/O_2$) was found in the same region of μ-1,2-peroxo diiron(III) intermediates in the related complexes with pendant pyridine or benzimidazole ligand systems. However, this blue intermediate exhibits EPR signals at g = 1.93, 1.76, and 1.59 at 4 K. These g values are characteristic of S = 1/2 system derived from an antiferromagnetically coupled high-spin Fe(II)Fe(III) units. **1** is the unique example of a (μ-alkoxo)diferrous complex which can bind dioxygen and form a metastable mixed-valence intermediate. At ambient temperature, most of $1/O_2$ intermediate decays to form a diamagnetic species. It suggests that the dacay reaction of the intermediate might be bimolecular, implying the formation of mixed-valence tetranuclear species in transition state.

Introduction

Dioxygen binding of the diferrous compounds has been of interest in recent years because of its relevance to iron-oxo proteins.[1] For example, diferrous sites of the reduced forms of hemerythrin (Hr),[2,3] ribonucleotide reductase (RNR),[4,5] and methane monooxygenase (MMO)[6,7] have been shown or postulated to interact with dioxygen and to be responsible for oxygen activation. DeoxyHr reversibly binds dioxygen to form oxyHr, characterized as a (μ-oxo)(μ-carboxylato)diiron (III) complex with a terminally bound hydroperoxide.[3,8] On the other hand, dioxygen reacts with reduced RNR and MMO irreversibly to afford oxidizing species capable of generating a catalytically essential tyrosyl radical and hydroxylating alkanes, respectively.[4~7]

A variety of diiron(III) complexes has been reported as structural and spectroscopic models for the inactive forms of the non-heme diiron proteins.[1,9] However, only a limited number of diiron(II) complexes have been reported as models for non-heme enzymes.[10~13] The chemistry of diiron(II) complexes are of importance to gain insight into the structures and functions of the active forms of the above metalloproteins, especially with respect to the binding mode and activation of dioxygen, and the oxygenation mechanism.

Although there are several μ-peroxo diiron complexes generated by the reaction of iron(III) complexes with hydrogen peroxide,[14] only a few iron(II) complexes which can bind O_2 in a μ-peroxo form have been known. For instance, complexes with (μ-alkoxo or hydroxo)(μ-carboxylato)diferrous cores such as $[Fe^{II}_2\{HB(3,5\text{-i-}Pr_2pz)_3\}_2(OH)(OBz)]$,[15,16] $[Fe^{II}_2(N\text{-Et-HPTB})(OBz)](BF_4)_2$,[17] and $[Fe^{II}_2(HPTP)(OBz)](BF_4)_2$[17b] bind O_2 to form (μ-1,2-peroxo)diiron(III) adducts. These complexes all have five-coordinate iron(II) centers with vacant sites for ligand binding, but O_2 binding is irreversible. By introducing methyl groups at the 6-positions of the pendant pyridines of HPTP, Hayashi *et al.* obtain $[Fe^{II}_2(Me_4\text{-TPDP})(OBz)(H_2O)](BF_4)_2$ which binds O_2 reversibly.[18]

In this paper, we report the properties of $[Fe^{II}_2(N\text{-Et-HPTB})Cl_2]BPh_4$ (**1**) which has a (μ-alkoxo)diiron(II) core unsupported by other bridges; this complex also binds dioxygen. We investigated the O_2 binding ability and activation process of diferrous complex by changing the Lewis acidity of the iron center *via* changing the ligand environment.

Experimental Section

Synthesis. The dinucleating ligand H-*N*-Et-HPTB was synthesized using the published procedures.[19] 1,2-Diaminobe-